



PROCEEDING
of
INTERNATIONAL COFERENCE
ON
PHYSICS EDUCATION
THROUGH
EXPERIMENTS

TIANJIN
CHINA



APRIL 23-27
1990

NEW EXPERIMENTAL ASPECTS OF TEACHING OPTICS

Werner B. Schneider, Didaktik der Physik - Physikalisches Institut Erlangen
Staudstr. 7, D - 8520 Erlangen

I.) INTRODUCTION

The aim of this lecture is to present some new ideas and experimental methods which can be useful in teaching optics. For this purpose we selected topics which can be treated without greater difficulties or special equipment, which represent a simplification of more complicated subjects, and which are not yet published in ordinary textbooks.

In the course of the lecture we present the following topics:

- a lens with an adjustable focal length,
- a new method of teaching holography,
- low cost retardation plates,
- a low cost interferometer to detect laser modes,
- an experiment to measure the refractive index using the overhead projector.

II.) A LENS WITH AN ADJUSTABLE FOCAL LENGTH

Lenses play an important role in teaching optics. In most applications lenses with a fixed focal length are used. Sometimes, however, it would be very useful to possess lenses with an adjustable curvature. With such a lens it is possible to show in a direct way that the focal length of a lens depends on the curvature of its surfaces and in addition it is an excellent model for the lens of the human eye.

For this purpose lenses had been developed in the past using transparent and flexible membranes for the surfaces of the lens and water as the refracting medium. The curvature of the membranes then can be regulated through the pressure of the water.

To our experience, however, this model lens is not sturdy enough to fulfil the rough conditions of laboratory work. Therefore we looked for another more suited method [1] and developed the experimental set-up which is schematically drawn on Fig. 1.

The idea of this method is to achieve a suitable curvature of a free water surface by means of an electric field which can be generated between the electrode E and the water surface. Since water molecules possess a large electric dipole moment they experience a force in the inhomogeneous electric

field. Therefore the surface is deformed up to an equilibrium between the electric force, the gravitational force, and the surface tension. The result is a mound-like deformation of the water surface opposite to the electrode. This curved surface region acts like a lens as can be proofed easily by forming images. The height of the "mound" and the corresponding curvature depend on the electric field strength which can be varied by the voltage U .

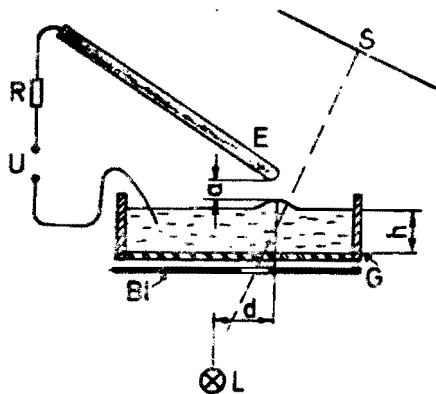


Fig. 1: Schematic drawing of the experimental set-up for the lens with an adjustable focal length.

E: electrode $\varnothing \approx 3-5\text{mm}$; h : thickness of the water layer ($h \approx 5-10\text{mm}$); a : distance between the water surface and the electrode ($a \approx 5\text{mm}$); R: resistor ($R \approx 100\text{M}\Omega$); U: adjustable high voltage up to 10 kV; B: diaphragm; L: light source which represents a bright object; G: vessel with a transparent bottom (e.g. metal ring $\varnothing \approx 10\text{cm}$ with a glass plate glued to one side); S: screen. For an object distance of 8 cm the image distance can be varied from 5 cm up to 3 m with a variation of the voltage U from 8.9 kV to 8.0 kV.

Normal laboratory equipment was used for the experimental set-up. Although it is not difficult to assemble the different parts it is nevertheless useful to optimize the set-up by varying the electrode distance a , the voltage U , and the displacement d . It turns out that the useful region of the "mound" which acts like a lens and produces good images is rather small (some mm^2). Therefore the lens has a small relative aperture, and one has to use bright objects for the formation of images. We found that the filament of the used light source suits very well.

The focal length can be varied from infinity to about 3 cm. The corresponding voltage U then varies from 0 to about 9 kV. The lower limit of the focal length is achieved when the necessary electric field strength is high enough to provoke an electric discharge between the electrode and the water surface. Concluding this part, the described experimental set-up is well suited to demonstrate in a direct way - even to a larger audience - that the focal length of a lens depends on the curvature of its surfaces.

In addition this method may be used to initiate the discussion of the formation of images through aspherical surfaces which is a current subject in technical optics.

Lit: [1] W. B. Schneider, "Ein einfaches, wenig bekanntes Verfahren zum Bau einer Linse mit variabler Brennweite". Physik und Didaktik 2, (1988) 158

III.) A NEW METHOD OF TEACHING HOLOGRAPHY

1. INTRODUCTION

Holography is a well known method of generating three-dimensional pictures, and even students are familiar to this new imaging process. Influenced by their experiences and observations with respect to holograms they are very interested to learn more about the physical background of holography. Therefore we were looking for a method of teaching holography from a very elementary point of view.

The main idea of this project [1] is to generate holograms of simple object-structures, i.e., one, two, three, ... etc. point sources arranged in a plane or in the space, which provide a stepwise introduction to the holographic method. Unfortunately, the production of real holograms of simple structures is rather difficult, and the teaching of the holographic recording and reconstruction process requires prerequisites which in general are not given in elementary physics courses. To overcome these difficulties we use a computer and a dot-matrix printer to simulate the holographic recording process.

2. HOW TO PRODUCE SUITED HOLOGRAMS

2.1. First step: The superposition of waves. In a first step we calculate the

superposition S of a plane reference wave and the respective spherical object wave(s) in the plane of the hologram (see Fig. 1). For the sake of simplicity we use the following approximations and assumptions:

- The phasor diagram in Fig. 2 shows the superposition S of the plane reference wave and one spherical object wave (simplest case) with the amplitudes A_0 and A_1 . It is evident, that in the case of $A_0 \gg A_1$ the magnitude of S can be expressed by the projection of S on A_0 . In practice we found that $A_0/A_1 \geq 3$ is already a good approximation.

- The amplitude of the spherical object wave depends on r , which is the distance between the point-

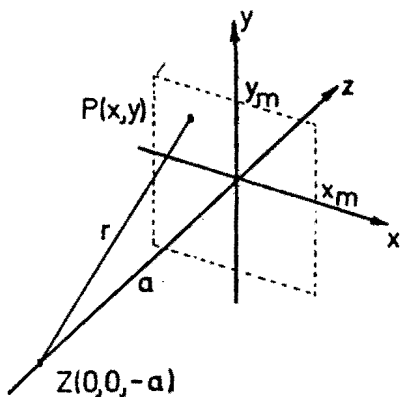


Fig. 1:

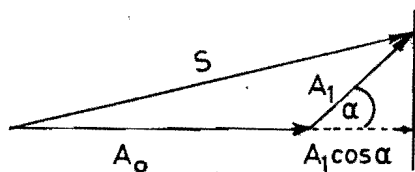


Fig. 2

source Z and the hologram point $P(x,y)$ (see Fig. 1). We assume the amplitude to be constant in the hologram plane. This is justified for r larger than the hologram dimensions.

- We neglect the term describing the time dependence in the wave equations and we choose the phase of the reference wave such that its amplitude is maximal in the hologram plane.

Considering these approximations and assumptions the superposition S , for example of a plane and a spherical wave at $P(x,y)$ in the hologram plane (see Fig. 1) can be written in the rather simple form:

$$S(x,y) = A_0 + A_1 \cos(2\pi r_1/\lambda) \quad (1)$$

where λ is the wavelength and $r_1 = \sqrt{a^2 + x^2 + y^2}$. The object wave is starting at $Z(0,0,-a)$.

For more object points arranged somehow in space the respective superposition is obtained in a similar way. For example, in the case of two point sources at $Z_1(x_0, 0, -a)$ and $Z_2(-x_0, 0, -a)$ in the x,y -plane parallel to the hologram plane the superposition is given by:

$$S(x,y) = A_0 + A_1 \cos(2\pi r_1/\lambda) + A_2 \cos(2\pi r_2/\lambda), \quad (2)$$

with $r_1 = \sqrt{a^2 + (x + x_0)^2 + y^2}$, $r_2 = \sqrt{a^2 + (x - x_0)^2 + y^2}$ and x_0 being the displacement in the x -direction.

2.2. Second step: Representing S on the monitor screen.

$S(x,y)$ is a continuously varying function which cannot directly be represented on the monitor screen or on a sheet of paper printed by a dot matrix printer, because both devices only allow a "digital" representation: either they print a dot or they do not. Therefore we describe $S(x,y)$ by the dot density on the screen or on the printer sheet. The number of dots per unit area is chosen proportional to S . The dots have to be randomly distributed in order to avoid additional regular structures in the simulated holograms.

To fulfill these two conditions we choose the probability of printing a dot proportional to $S(x,y)$ (for $A_0 = 3$ and $A_1 = 1$ in equ. (1), e. g., the respective probability is $S/4$). A dot is printed when a random number between 0 and 1 is smaller than the respective normalized value of S as indicated in the following BASIC program line:

```
IF RANDOM < S(x,y)/4 THEN PLOT P(x,y).
```

For $S(x,y)/4 \approx 1$ the probability for printing a dot is rather high, nevertheless it is possible that the respective random number is larger than $S/4$ and that the dot is not printed. This apparent error, however, is compensated over a larger area due to the random distribution of the dots and it proofs that the number of dots per unit area is proportional to S .

In the calculations all lengths are expressed in an arbitrary unit LU, which is determined by the minimum dot separation $LU = 0,4\text{mm}$ for our printer. Good results are obtained for $a \approx 5000LU$, $\lambda \approx 2LU$ and $x_0 \approx 100LU$.

Fig. 3 represents the results of the simulation for some representative examples which allow a stepwise introduction to holography. In all examples we assumed a plane reference wave. Fig. 3a shows the pattern for one spherical object wave. This pattern (Fresnel zone plate) is the basis of all holograms. In the following examples the calculation is restricted to one quarter of the hologram plane (Fig. 1) in order to get higher resolutions. Fig. 3b illustrates the result for two spherical object waves. The respective object points are located in a plane parallel to the hologram plane. It shows two overlapping Fresnel zone plates. Fig. 3c illustrates the pattern for two spherical object waves with the object points located on a straight line vertical to the hologram plane. We observe two concentric Fresnel zone plate systems. Fig. 3d is similar to Fig. 3b with the difference that the amplitudes of the two spherical waves are not equal (ratio 1:2). Fig. 3e shows the pattern for six object points arranged as the corner-points of a prism (two planes parallel to the hologram plane and each plane with 3 points). With the knowledge of the structures in Fig. 3a to 3d it is possible to recognize the respective arrangement of the points from the pattern structure itself. Fig. 3f shows the pattern in the case of one plane object wave (object point located at infinity). The result is a grating structure. Fig. 3g shows the pattern for two plane object-waves starting under two different directions at infinity. Fig. 3h represents the simulation for a cylindric object wave, which comes from a slit located in front of the hologram. This pattern helps us to explain the transition from a grating to a Fresnel zone plate structure.

The resolution of these examples is set to the relative low value of 400×470 dots per chosen sector of the hologram plane, which is not sufficient to get good results, but is more suited for the reproduction. To get holograms of good quality we had to set the resolution to about 3600×2400 dots for the same sector (Fig. 3b - 3h). For this purpose we split the respective sector of the hologram plane in 24 parts, calculated the superposition of the respective wave configuration for each part, made a hardcopy of the screen, and finally glued the sheets in the right order to get a large pattern of about $(1.2 \times 0.8) \text{m}^2$ with approximately $8.6 \cdot 10^6$ dots and the desired resolution.

2.3. Third step: Photographic reduction.

The large patterns have to be reduced photographically in order to get transparencies similar to "real" holograms. For this purpose we used an ordinary

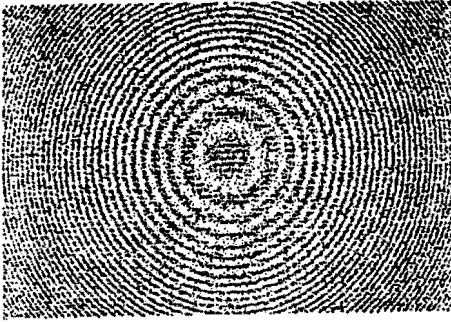


Fig. 3a)

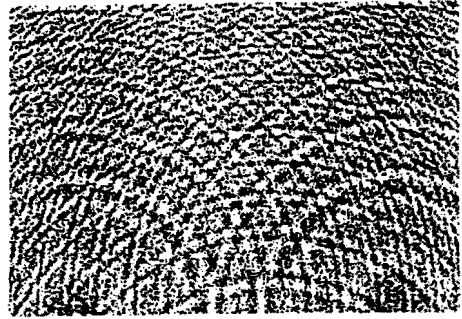


Fig. 3e)

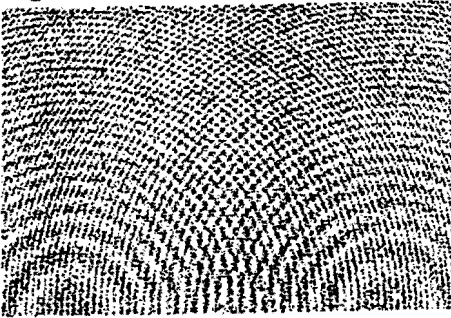


Fig. 3b)

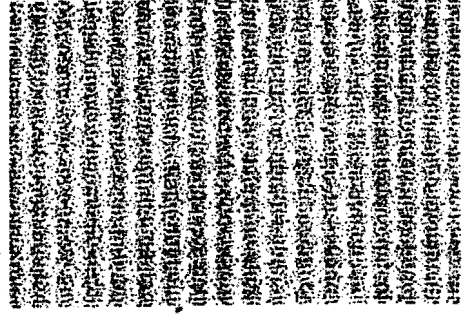


Fig. 3f)



Fig. 3c)

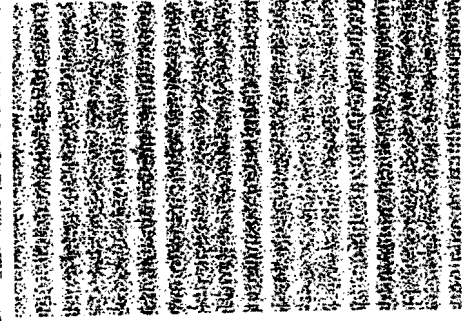


Fig. 3g)



Fig. 3d)

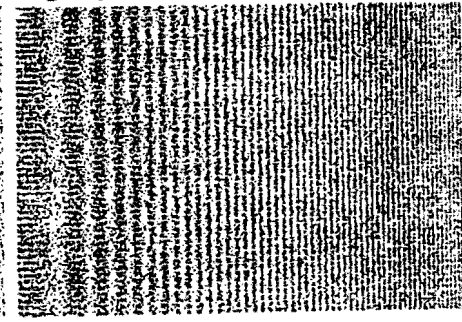
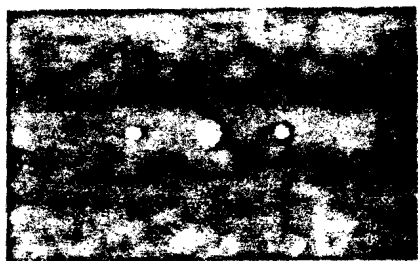


Fig. 3h)

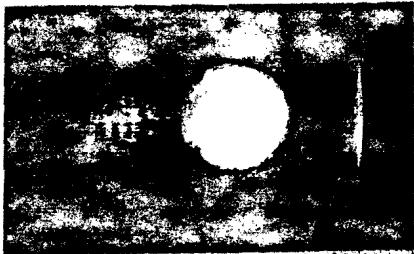
amateur camera (film format 24mm x 36mm) and a high resolution black and white negative film (e.g. Agfapan professional 25 ASA, resolution 350 lines/mm). The exposure and the developing time was chosen such that the photographic process is approximately "digital" in order to get a point-by-point recording, i. e., each dot gives a well separated "hole" in the film emulsion. We found the reduction 1 : 30 to 1 : 50 sufficient to get structures which are still resolved on the film, and show already diffraction effects.

2.4. Fourth step: The reconstruction.

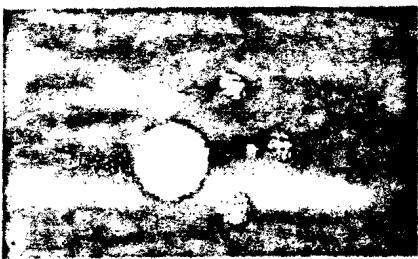
Holograms have many properties of a grating and the reconstruction of the hologram images is similar to a diffraction experiment with a grating. The experimental set-up is described in ordinary optic textbooks (e.g., [2, 3]). Fig. 4 illustrates by photographs some results of the reconstruction process with different object-point arrangements.



4a



4b



4c



4d

Fig. 4: Examples for the reconstructed images.

Fig. 4a represents the reconstructed image of the hologram pattern in Fig. 3f (a linear grating) and shows the surprising effect that only the zero and first refraction order appear. This proves that the simulation process gener-

ates a sinusoidal transmission structure on the film (negative). This result is rather important from the technical point of view and it simplifies the application of the simulated holograms in the teaching process.

From the calculation which leads to the hologram in Fig. 3f we expect only one point at infinity. The respective reconstruction in Fig. 4a, however, shows two points - one at "plus" and one at "minus" infinity. This ambiguity is due to the neglected time dependence in the wave description. In equ. (1) for instance it is impossible to distinguish between "incoming" and "outgoing" waves which gives rise to the two images in the reconstruction, the a real and the virtual (conjugate) image [2, 3].

Fig. 4b shows the reconstruction of the image based on the hologram in Fig. 3h which represents the superposition of a plane and a cylindric wave (a slit placed at a finite distance to the hologram plane). The real image (slit) on the right side is in focus; the virtual image of the slit appears out of focus on the left side.

Fig. 4c shows the reconstruction of a real three-dimensional point arrangement (tetrahedron, hologram pattern in Fig. 3e). The three-dimensional character is demonstrated by focusing on the point on the top of the tetrahedron. The other three points originally arranged in a plane parallel to the hologram plane are out of focus - as expected. In Fig. 4d we have chosen another camera position and another diaphragm. The view of the tetrahedron has changed. This change of the perspective is another test for the three-dimensional character of the reconstructed images. In addition all points of the tetrahedron appear approximately in focus on this photo. This effect indicates that the depth of focus increases when the diameter of the diaphragm decreases: an observation well known from real holograms.

3. ADDITIONAL REMARKS:

The simulation of holograms for simple object point structures allows a step-wise introduction to holography. Contrary to usual methods of teaching holography, the described method requires only the mathematical description of waves in its simplest form and Huygens' principle: the simulated holograms represent different dot distributions, and after the photographic reduction the transparencies show a respective hole distribution. Both properties allow the application of Huygens' principle to explain holography: the dots represent "frozen" single point sources and their distribution the frozen wavefront. The holes in the transparency can be regarded as single point sources which can be reactivated. When shining light on the transparency each hole becomes a

source of spherical wavelets and the envelope of these wavelets represents the reactivated wavefront just after the hologram plane.

Testing this method with students we noticed an aspect which should be mentioned: the students liked to do something reasonable with the computer and they found it very motivating to do some practical work as glueing, taking photos and developping films to produce the holograms. Both aspects yield new motivation for other subjects in physics.

4. REFERENCES:

- [1] H. Dittmann, W. B. Schneider, "Computererzeugte Interferenzmuster als Zugang zur Holographie", Physik und Didaktik 3, 1988 (207-216)
- [2] E. Hecht "Optics", Reading 1987
- [3] M Françon, "Holographie", Berlin 1972

IV.) LOW COST RETARDATION PLATES

This subject has been already presented at the TMP-Conference in 1988 [1]. Therefore only the idea of this method will be presented here.

Lucite (Plexiglas) (manufacturer: Röhm, Postfach 4242, D - 6100 Darmstadt) has some exceptional properties which makes it very interesting for teaching optics. It is optically anisotropic, it scatters laser light, it is cheap, it has a high transparency for light, and it is easily being cut and polished.

Here we are especially interested on the anisotropic behaviour of Plexiglas rods. This property is a consequence of the special fabrication process which induces a rather small birefringence (constant, uniaxial) with the optical axis perpendicular to the axis of the rod. The difference Δn between the principal refraction indices is very small, $\Delta n \approx 10^{-5}$. Therefore linear polarized light with the E-vector oriented under 45° to the optic axis will be transformed to elliptical polarized light along its path through the rod. As Δn is rather small the phase shift $\delta = \Delta n 2\pi d/\lambda$ varies rather slowly with the path length d . Therefore, e. g., the phase shift $\pi/4$ ($\lambda/4$ -retardation) takes place on the relativ long path length $d \approx 9\text{mm}$. If a laser beam is used this transformation can easily be observed via the scattered light. This property is very suitable for teaching and understanding how retardation plates work. It is evident that $\lambda/4$ - or $\lambda/2$ -retardation plates can be obtained in a very simple way using this material. One has only to cut the rod at the desired length and to polish the surfaces. In addition to the simple fabrication, these retardation plates are easy to handle, they are adjusted to the given wavelength, and they represent zero order retardation plates which are normally very expensive.

In optic courses at our university every student has to fabricate his own re-

tardation plates. We found out that this activity is a good supplement to the ordinary laboratory work and it offers the possibility to get a deeper insight and understanding of optical birefringence.

Lit.: [1] W. B. Schneider: "A surprising property of plexiglass rods and its application to experiments". In: Proceedings of the TMP - Conference (Condensed Matter) 1988, ed. K. Luchner et al. ; Singapore 1989

IV.) A LOW COST INTERFEROMETER TO DETECT AXIAL LASER MODES

Plates of Plexiglas have another remarkable property: the surfaces are nearly optically flat and nearly parallel to each other. Thus, they can be used even in an interferometer device which first was described by Pohl [1]. The idea of this interferometer is shown in Fig. 1a. It is an amplitude splitting interferometer where the splitting is achieved in a very simple way: the beam reflected on the front surface has nearly the same amplitude as the beam reflected on the back surface as can be proofed easily (neglecting absorption losses). The disadvantage of this method is that only 4% of the incoming light takes part on the interference process. With a bright point source, however, it is possible to project the ring system even to a larger screen in a lecture hall [1] and to make it visible for a larger audience. It is evident that this amplitude splitting device is much cheaper and simpler as the a half silvered mirror used in a Michelson interferometer as a beam splitter.

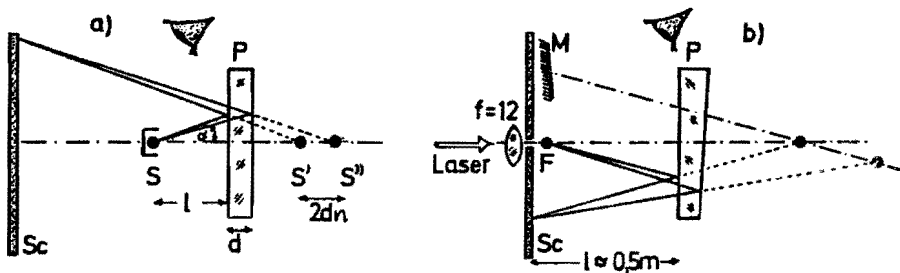


Fig. 1: a) Pohl interferometer (P: plate of thickness d ; S: point source; S' and S'' virtuell lightsources with the distance $2dn$; n : refractiv index of the plate; Sc: screen)
 b) Pohl interferometer illuminated by a laser. The surfaces of the plate P are not perfectly parallel to each other (Plexiglas). (M: Mirror; F: focal point as piont source)

In the original version of the Pohl interferometer rather thin plates of mica and a mercury lamp are used. For thicker plates it requires a bright point

source with a longer coherence length.

Therefore we used a He-Ne-laser. Its beam passes through a lens with a small focal length ($f \approx 1\text{cm}$) and then the focus serves as the point source (see Fig. 1b). We tried different plates of glass and of Plexiglas in order to see whether the surfaces are "good" enough to get a concentric ring system even for thicker plates. We found that plates of Plexiglas suites very well. We noticed only a small inclination of the surfaces which doesn't affect the form of the ring system but shifts its center out of the optic axis, as indicated on Fig. 1b. This is rather advantageous since this property allows to reflect the ring system with a small mirror on a screen. This is essential in the case of thicker plates where the diameter of the ring system becomes rather small otherwise.

The spectral resolution increases with the path difference Δs of the interfering beams [1]; $\Delta s \approx 2dn$ for $\alpha \approx 0$ (n : refractive index of the plate; α : angle of aperture). Therefore we tried thicker plates. Since the thickness of the plates of Plexiglas available was limited to 2cm, some plates were glued together, thus reaching values up to 6cm. To get a good transparency we used immersion oil which has a refractive index similar to that of Plexiglas. For values d smaller than 4cm the ring system is always sharp. For $d = 6\text{cm}$ we observe something fascinating: The ring system changes its sharpness from time to time and sometimes it vanishes totally. This indicates that the spectral resolution of this interferometer is already high enough to allow the detection of laser modes in a qualitative way. For $d = 6\text{cm}$ the optical path difference is about 18cm and the maximum of one laser mode begins to coincide with the adjacent minimum of the other laser mode. Therefore the contrast of the ringsystem is rather reduced. The laser modes change their frequency and amplitude through thermal effects in the laser cavity. As a consequence one observes the appearance and disappearance of the ring system. The difference of the wavelengths $\Delta\lambda$ for adjacent modes is [III.1]:

$$\Delta\lambda = \lambda^2/2l \approx 6,7 \cdot 10^{-4} \text{ nm} \quad (l: \text{length of the laser cavity, here } l = 30\text{cm}).$$

The resolving power $\lambda/\Delta\lambda$ then is about 10^6 which is one order of magnitude better than that of a good grating spectrometer with a maximal resolution of 10^{-2} nm [III.1].

In conclusion, the great advantages of this type of interferometer for teaching are evident: The interference fringes can be projected and thus be shown to a larger audience, no complicated adjustments are needed, and it is extremely cheap compared to other interferometer devices having the same spectral resolving power which allows the detection of laser modes.

V.) A SIMPLE METHOD TO MEASURE THE REFRACTIVE INDEX

It is well known that the image of an object point situated in an optically more dense material seems to be lifted if viewed at through a boundary surface from an optically less dense material (e.g. air to water). This situation is schematically illustrated in Fig. 1.

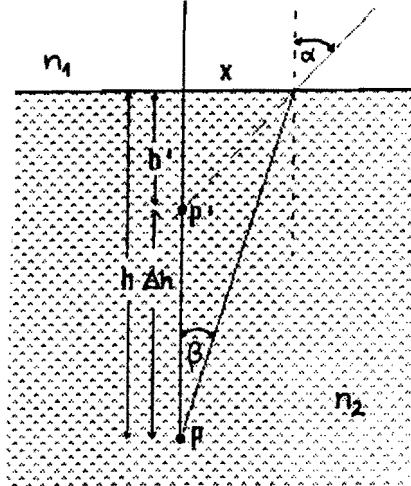


Fig. 1: Schematic drawing to explain the determination of the refractive index

Denoting with n_2 the index of refraction of the optically more dense material it follows from Fig. 1 for angles of incidence $\alpha \ll 10^\circ$:

$$n_2 = \frac{\sin \alpha}{\sin \beta} \approx \frac{\tan \alpha}{\tan \beta} = \frac{h}{h'} = \frac{h}{h - \Delta h}. \quad (1)$$

Usually the thickness h is known, and from a measurement of Δh the unknown refractive index n_2 can be determined with equation (1).

This measurement can be carried out in a nice way with the overhead projector: First the image of a transparency is focused by the projector. Then the unknown material is placed on the center of the projector table onto the transparency. As a consequence the image becomes defocused, and one has to lift the lens of the projector by an amount of Δh to refocus the image. This displacement of the lens is easily measured and one gets n_2 with equation 1. The condition $\alpha \ll 10^\circ$ is fulfilled for common lenses (for $f = 35\text{cm}$ and $\varnothing = 5\text{cm}$ one gets $\alpha_{\max} \approx 4^\circ$).

In addition to the determination of refractive indices this method may initiate a more general discussion about the formation of images by a flat boundary surface [1].

Lit.: [1] H. Dittmann, W. B. Schneider: "Mit dem Computer ins Aquarium geschaut". In: "Wege in der Physikdidaktik" (ed. W. B. Schneider), Palm und Enke, Erlangen 1989